



Norwegian
Meteorological
Institute

METreport

No. 04/2022
ISSN 2387-4201
Free

Notes on 1991–2020 wind speed climatology

based on NORA3 near-surface data

Cristian Lussana, Inger Hanssen-Bauer, Jan Erik Haugen, Andreas Dobler,
Hans Olav Hygen, Anita Verpe Dyrddal and Hilde Haakenstad

The Norwegian Meteorological Institute, Oslo, Norway



Credit: Maria Scheel (distributed via imaggeo.egu.eu)



Norwegian
Meteorological
Institute

METreport

Title Notes on 1991–2020 wind speed climatology	Date March 3, 2022
Section Division for Climate Services	Report no. 04/2022
Author(s) Cristian Lussana, Inger Hanssen-Bauer, Jan Erik Haugen, Andreas Dobler, Hans Olav Hygen, Anita Verpe Dyrørdal and Hilde Haakenstad	Classification <input checked="" type="radio"/> Free <input type="radio"/> Restricted
Abstract The 1991–2020 climatology of the wind speed field is studied, with particular attention to the characterization of strong wind events. The data source used is the high resolution NORA3 reanalysis. The domain includes the Norwegian mainland, the North Sea, the Norwegian Sea, and the Barents Sea.	
Keywords climatology, wind speed, NORA3, Norway	

Disciplinary signature
Hans Olav Hygen

Responsible signature
Cecilie Stenersen

Contents

1	Introduction	4
2	Methods	5
2.1	Climate normals and indices	5
2.2	Temporal trends	5
3	Wind speed climatology over land	6
3.1	Annual aggregated variables	6
3.1.1	Temporal trends	10
3.2	Monthly aggregated variables	12
3.2.1	Temporal trends	15
4	Wind speed climatology over the sea	20
4.1	Annual aggregated variables	20
4.1.1	Temporal trends	23
4.2	Monthly aggregated variables	25
4.2.1	Temporal trends	28
5	Conclusions	33

1 Introduction

The study of the 1991–2020 climatology of near-surface wind speed over Norway is the topic of this report. The aims are to characterize the distribution of wind speed values, its spatial patterns and to study the possible presence of temporal trends. The results obtained can also be useful for civil protection purposes and for the planning of wind energy production.

The two variables considered are 10–metre and 100–metre wind speed (i.e. wind speed at altitudes of 10 m and 100 m above the ground). The latter variable is commonly used in applications related to energy production.

The data source used is the Norwegian Reanalysis (NORA3, *Haakenstad et al.*, 2021), that is a dynamical downscaling of the global reanalysis ERA5 (*Hersbach et al.*, 2020) over Fennoscandia, the North Sea, the Norwegian Sea, and the Barents Sea. The model used for the downscaling is a state-of-the-art nonhydrostatic numerical weather prediction model and the original data are made available on a regular grid having 3 km as spacing in both zonal and meridional directions. The data used in this study have been re-projected onto a 1 km grid by means of bilinear interpolation. Our elaborations are based on the hourly wind speed, that is the instantaneous wind speed made available as one value per hour. As stated in the paper by *Haakenstad et al.* (2021) "The wind field is greatly improved relative to its host analysis (i.e. ERA5), in particular in mountainous areas and along the improved grid-resolving coastlines". In the same paper, the authors performed an extensive evaluation of the hourly 10–m wind speed of NORA3 against in-situ observations from reference stations, where they show that NORA3 satisfactorily reproduces the observed values, both the average values and the higher percentiles.

The 30-year time period from 1991 to 2020 is considered in our analysis. The wind climatology is characterized by means of climate normals and a limited number of climate indices. The wind speed temporal trends are calculated on a grid point by grid point basis and the statistical significance of each of the trends is assessed.

The wind over the land and over the sea are treated separately in the report, since the characteristics of the fields are rather different over the two surfaces. Over land, the wind speed is generally lower than on the sea. Besides, over land the wind speed is much more variable in space, especially over Norway, since it is affected by the roughness of the terrain.

The most significant findings of our analysis are included in this report. A further

document includes many other figures, which may be of interest to some readers. The additional document with the *Supporting material* is also freely available as a MET Norway report.

The document is organized as follows. Sec. 2 summarizes the elaborations made and the implementation choices. Sec. 3 describes the climatology of wind speed over land. Sec. 4 describes the climatology of wind speed over the sea. Sec. 5 summarizes the main messages of the document. The data access is then described in the Appendix.

2 Methods

2.1 Climate normals and indices

A climate normal, often abbreviated as "normal", of a particular variable is defined as the 30-year average. For example, the average wind speed normal in June for the city of Stavanger would be computed by taking the average of the 30 June values of monthly averaged wind speeds from 1991 to 2020. Each of the 30 monthly values was in turn derived from the daily averaged wind speed at Stavanger.

The climate indices considered are: the 99-th percentiles of the wind speed computed both on an annual and on a monthly basis; the number of hours in a year with wind speed above or below predefined thresholds.

2.2 Temporal trends

As stated above in the Introduction, the wind speed temporal trends are calculated on a grid point by grid point basis and the statistical significance of each of the trends is assessed.

The gridded fields considered in the calculations are annual or monthly aggregated quantities, such as averages or the 99-th percentiles. Usually, the trends indicate the rate of variation of these quantities as m/s per decade over the period 1991–2020. However, the results are presented in this document as normalized trends, that is the rates of variation divided by the corresponding normals.

At each grid point, the method implemented for the estimation of the rate of variation is the Theil-Sen linear regression as described by *Wilks* (2019) (p. 283). This method is also known as the median of pairwise slopes and it is characterized as an efficient (i.e. good performances relative to the standard "least-squares regression") and resistant (i.e.

insensitive to misbehaviour of the data) method (*Lanzante, 1996*).

Are the trends significant with respect to the null hypothesis of no trend in the data? The answer to this question is obtained at each grid point by applying the Mann-Kendall trend test (*Wilks, 2019*) (p. 178) to the corresponding timeseries. For each point, the Mann-Kendall trend test returns a p value, that is the probability of obtaining test results at least as extreme as the results actually observed, under the assumption that the null hypothesis is correct. In particular, we apply a two-tailed significance test because the alternative hypothesis we consider is that of having either an upward or downward monotonic trend. [Note that if the alternative hypothesis was that of an upward only (or downward only) trend then we could have used a one-tailed test.] if we were dealing with a single time series, it would have been enough for us to define the threshold $\alpha = 0.10$ (or 10%) and reject the null hypothesis of no trend at level of significance α when the p value was smaller than α . However, we are dealing with a collection of multiple tests and the spatial correlation in the underlying gridded data induces statistical dependence among the local tests, which is one of the cases treated in the book by *Wilks (2019)* (p. 198). In multiple testing problems, the data being tested are the result of "local" tests, and the "global" null hypothesis is that all the local null hypotheses (of no trend) are true. The false discovery rate (FDR) approach (or Benjamini-Hochberg meta-test) provides a method to reject the global null hypothesis at level α_{global} , which we set such that $\alpha_{\text{global}} = \alpha = 0.10$. In practice, the FDR approach adjusts the local p values and the null hypothesis is rejected at level α_{global} for all those points where the adjusted local p values are smaller than $\alpha_{\text{FDR}} = 2\alpha_{\text{global}}$.

3 Wind speed climatology over land

3.1 Annual aggregated variables

The results are presented in the figures that follows, either in this section (Figs. 1– 2) or in the supporting material (SFIGs. 1– 6). For convenience, the list of available figures is shown below:

- Fig. 1. Average 10–metre wind speed 1991–2020 normal. Each of the 30 annual values was derived from NORA3 hourly 10–metre wind speed.
- SFIG. 1. 30-year average (1991–2020) of the 99-th percentile of the annual 10–

metre wind speed. Each of the 30 annual values was derived from NORA3 on the basis of all daily mean 10-metre wind speeds.

- Fig. 2. Average 100-metre wind speed 1991–2020 normal. Each of the 30 annual values was derived from NORA3 hourly 100-metre wind speed.
- SFig. 2. 30-year average (1991–2020) of the 99-th percentile of the annual 100-metre wind speed. Each of the 30 annual values was derived from NORA3 on the basis of all daily mean 100-metre wind speeds.
- SFig. 3. 30-year average (1991–2020) of the number of hours in a year with 10-metre wind speed less than 2 m/s. Each of the 30 annual values was derived from NORA3 on the basis of all hourly 10-metre wind speeds.
- SFig. 4. 30-year average (1991–2020) of the number of hours in a year with 10-metre wind speed greater than 20 m/s. Each of the 30 annual values was derived from NORA3 on the basis of all hourly 10-metre wind speeds.
- SFig. 5. 30-year average (1991–2020) of the number of hours in a year with 100-metre wind speed less than 4 m/s. Each of the 30 annual values was derived from NORA3 on the basis of all hourly 100-metre wind speeds.
- SFig. 6. 30-year average (1991–2020) of the number of hours in a year with 100-metre wind speed greater than 25 m/s. Each of the 30 annual values was derived from NORA3 on the basis of all hourly 100-metre wind speeds.

The layout of all figures is the same or very similar. The left panel shows a map with the field of the normal values over a regular grid with spacing of 1 km. The colour scale is defined on the basis of the percentiles of the distribution of values. For instance, for Fig. 1, the range of values is divided into 18 intervals. The first interval ranges from the minimum value (1.32 m/s) to the value of (approximately) the 6-th percentile (2.16 m/s), then the second interval includes the slightly higher values, up to the 12-th percentile (2.41 m/s) and so on. The greatest value in the legend is the maximum value of the field. For the figures referring to normal values or the 99-th percentile, the list of percentiles reported in the legend is: the minimum value; the 6-th; the 12-th; the 18-th; the 24-th; the 29-th; the 35-th; the 41-st; the 47-th; the 53-rd; the 59-th; the 65-th; the 71-st; the 76-th; the 82-nd; the 88-th; the 94-th and the maximum value. For the figures referring to the

climate indices, the list of percentiles reported in the legend is: the minimum value; the 10-th; the 20-th; the 30-th; the 40-th; the 50-th; the 60-th; the 70-th; the 80-th; the 90-th and the maximum value. Besides, for climate indices, the reddish colors are always used to indicate regions where the wind speed is stronger, while the bluish colors indicates regions where the wind is weaker.

The right panel shows the normal values as a function of the elevation classes using box-and-whisker plots. Each box-and-whiskers plot represents the distribution of field values in a specific elevation class and it is made of: a light-gray box that extends from the 25-th percentile to the 75-th percentile, the median is marked with a thick line; the whiskers extend out from the box to the most extreme data point which is no more than 1.5 times the interquartile range; the points mark the outliers. The 100-meter elevation classes are labelled with the highest elevation in the class, such that e.g. "100 m" indicates grid points with elevations from 1 m to 100 m. An exception is class "0 m", which includes only points having elevation equal to 0 m.

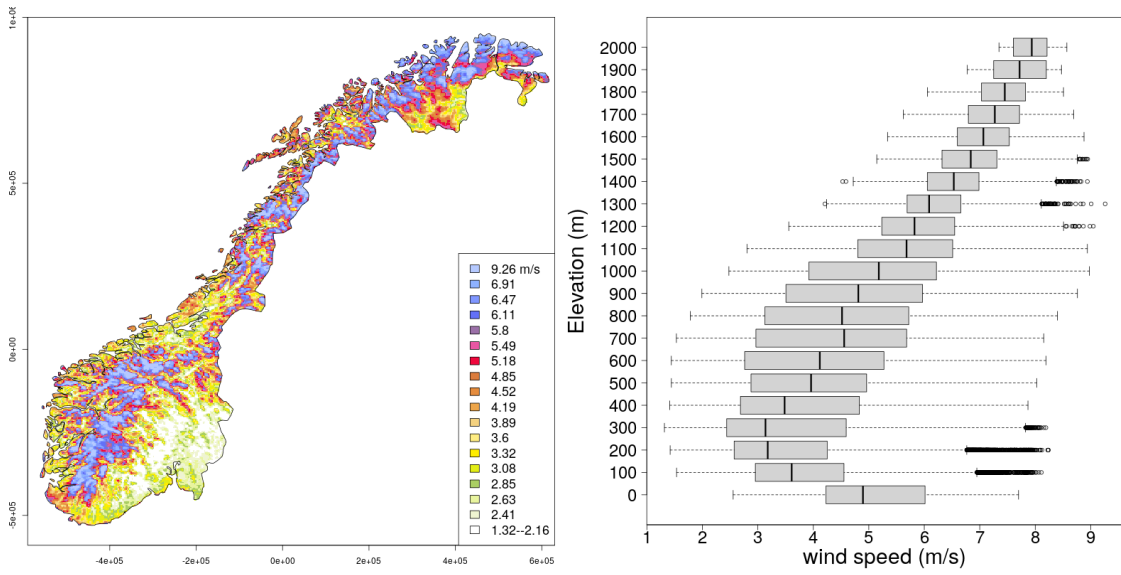


Figure 1: Average 10–metre wind speed 1991–2020 normal. Each of the 30 annual values was derived from NORA3 hourly 10–metre wind speed.

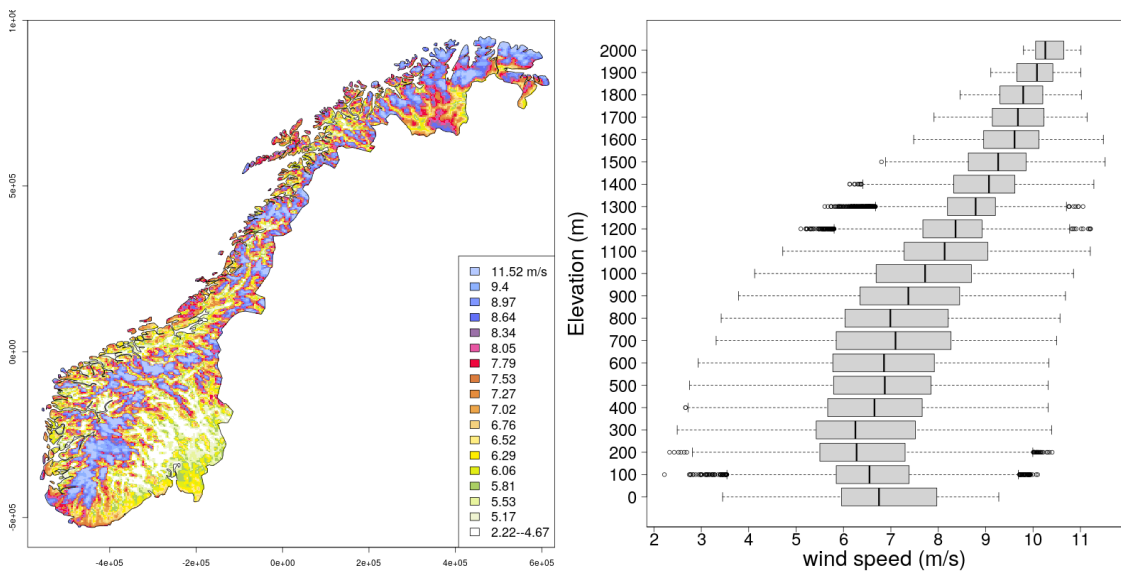


Figure 2: Average 100–metre wind speed 1991–2020 normal. Each of the 30 annual values was derived from NORA3 hourly 100–metre wind speed.

3.1.1 Temporal trends

The results are presented in the figures that follows, either in this section (Figs. 3– 4) or in the supporting material (SFIGs. 7–32). For convenience, the list of available figures is shown below:

- Fig. 3. Normalized linear trends of the annual averaged 10–metre wind speed over the period 1991-2020. At a grid point, each of the 30 annual values used was derived from NORA3 hourly 10–metre wind speed.
- SFIG. 7. Normalized linear trends of the annual 99-th percentile of the 10–metre wind speed over the period 1991-2020. At a grid point, each of the 30 annual values used was derived from NORA3 daily averaged 10–metre wind speed.
- SFIG. 8. Normalized linear trends of the annual averaged 100–metre wind speed over the period 1991-2020. At a grid point, each of the 30 annual values used was derived from NORA3 hourly 100–metre wind speed.
- Fig. 4. Normalized linear trends of the annual 99-th percentile of the 100–metre wind speed over the period 1991-2020. At a grid point, each of the 30 annual values used was derived from NORA3 daily averaged 100–metre wind speed.

A comparison with station data has been performed and a selection of results is shown in the Supporting material (SFIGs. 9–32).

The layout of all figures of the section is the same. The left panel shows a map with the normalized rate of variation of the wind speed per decade (i.e. the ratio between the slope of the Theil-Sen linear regression and the normal value) over a regular grid with spacing of 1 km. The units of the rate of variation are % of the climate normal per decade. The colour scale is symmetric around 0 %. Bluish colors indicate a decrease in wind speed over time. Reddish colors indicate an increase in wind speed over time. The green colors mark those regions where the wind speed is almost constant over the years.

The right panel indicates where the temporal trends are significant at the 10% level. Note that nowhere are trends significant at the 5% level.

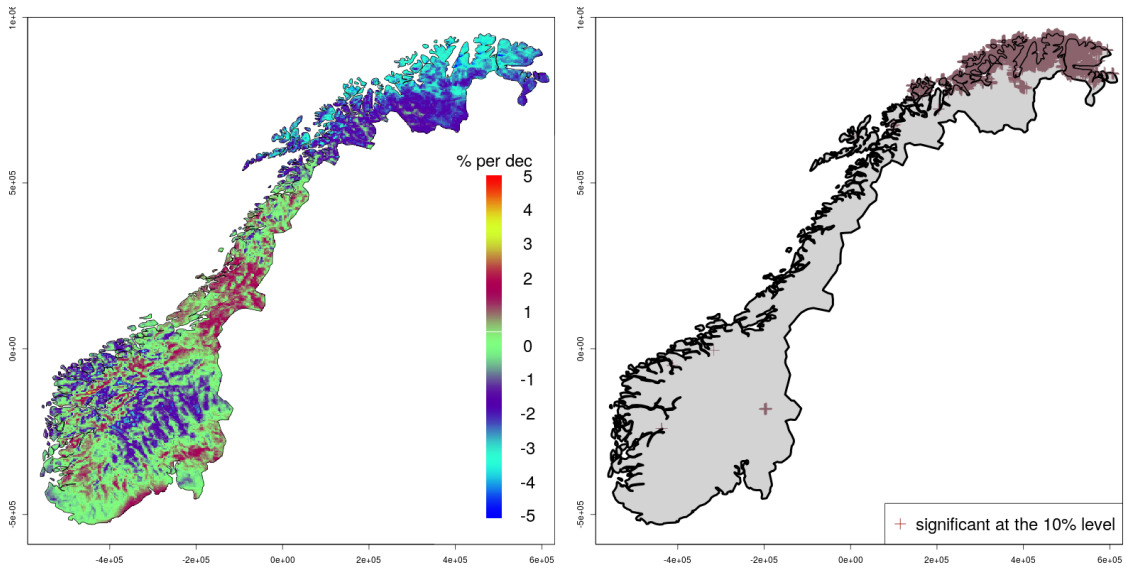


Figure 3: Normalized linear trends (in % of the climate normals per decade) of the annual averaged 10–metre wind speed over the period 1991-2020. At a grid point, each of the 30 annual values used was derived from NORA3 hourly 10–metre wind speed. The left panel shows the map of the normalized trends. The right panel shows the grid points where the temporal trends are significant at the 10% level.

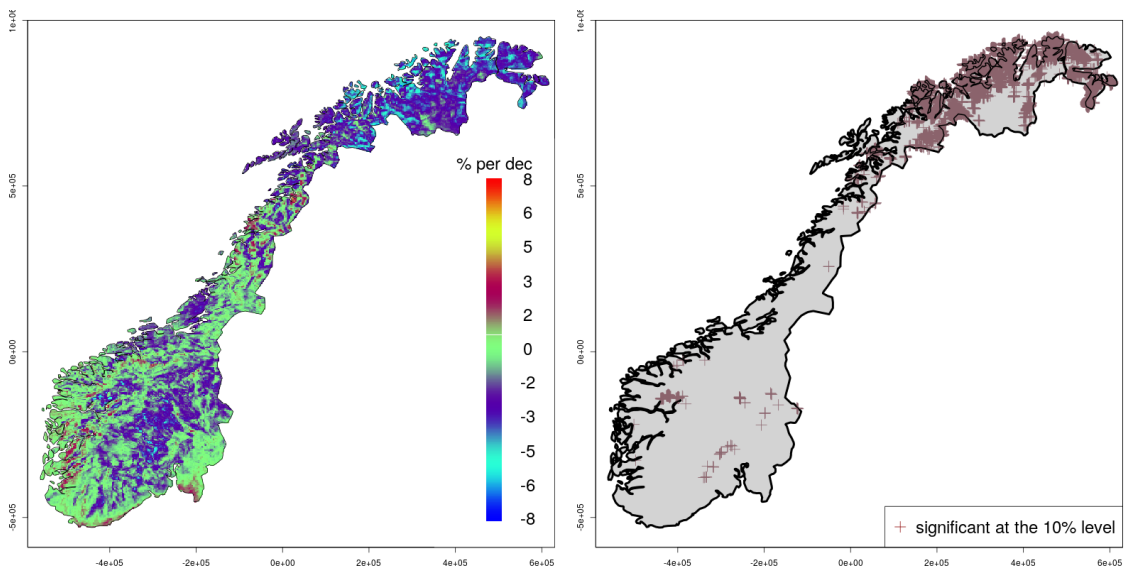


Figure 4: Normalized linear trends (in % of the climate normals per decade) of the annual 99-th percentile of the 100–metre wind speed over the period 1991-2020. At a grid point, each of the 30 annual values used was derived from NORA3 daily averaged 100–metre wind speed. The left panel shows the map of the normalized trends. The right panel shows the grid points where the temporal trends are significant at the 10% level.

3.2 Monthly aggregated variables

The results are presented in the figures that follows, either in this section or in the supporting material (SFigs. 33– 40). For convenience, the list of available figures is shown below:

- Fig. 5. Average 10–metre wind speed 1991–2020 monthly normals. Each of the 30 annual values was derived from NORA3 hourly 10–metre wind speed.
- Fig. 6. Average 100–metre wind speed 1991–2020 monthly normals. Each of the 30 annual values was derived from NORA3 hourly 10–metre wind speed.

The layout of the figures is similar to those of the maps in Sec. 3.1.

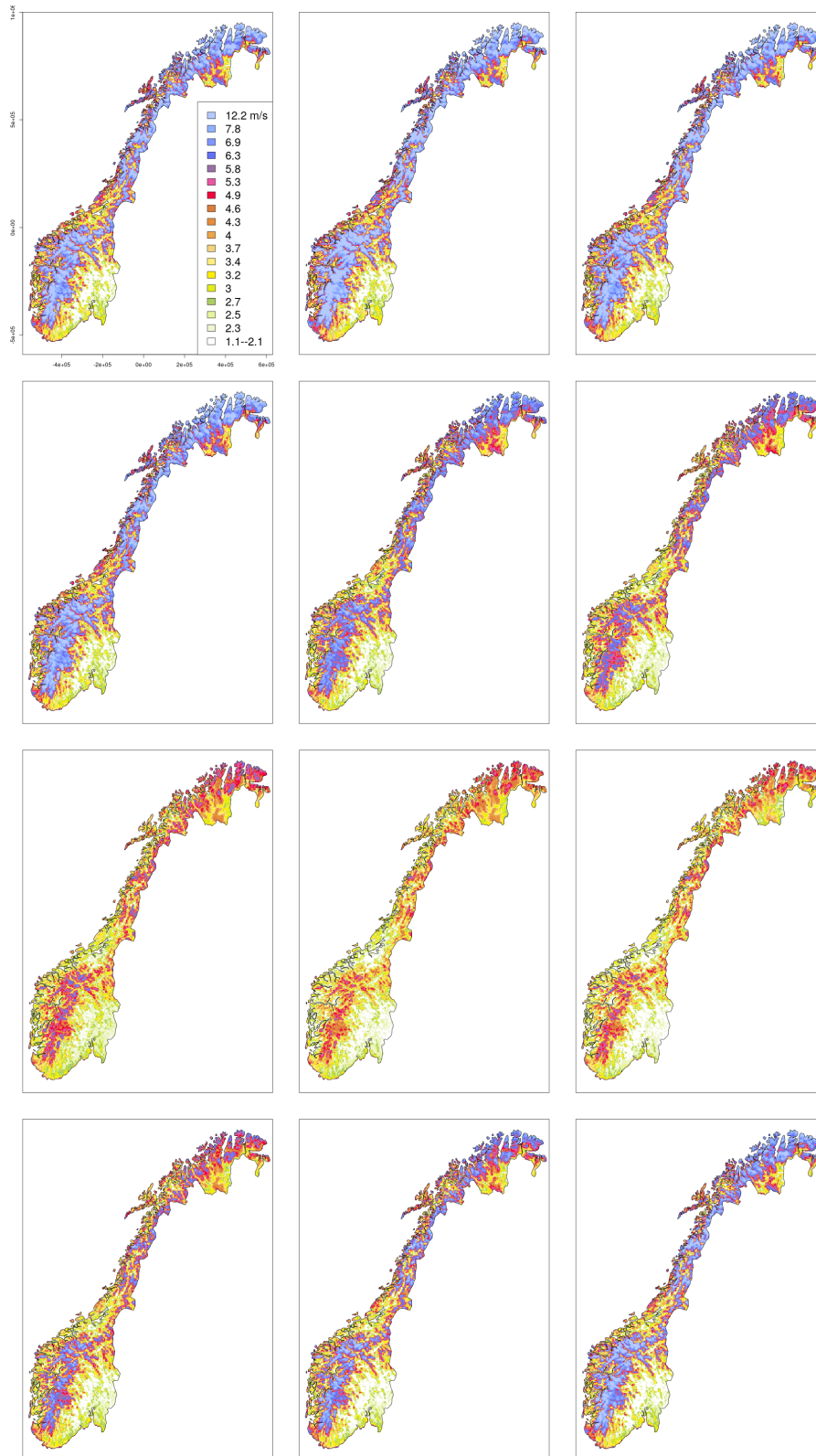


Figure 5: Average 10-metre wind speed 1991–2020 monthly normals. Winter months in the top row (left to right): Dec, Jan, Feb (or DJF). Spring in the 2nd row (MAM). Summer in the 3rd row (JJA). Autumn in the bottom row (SON).

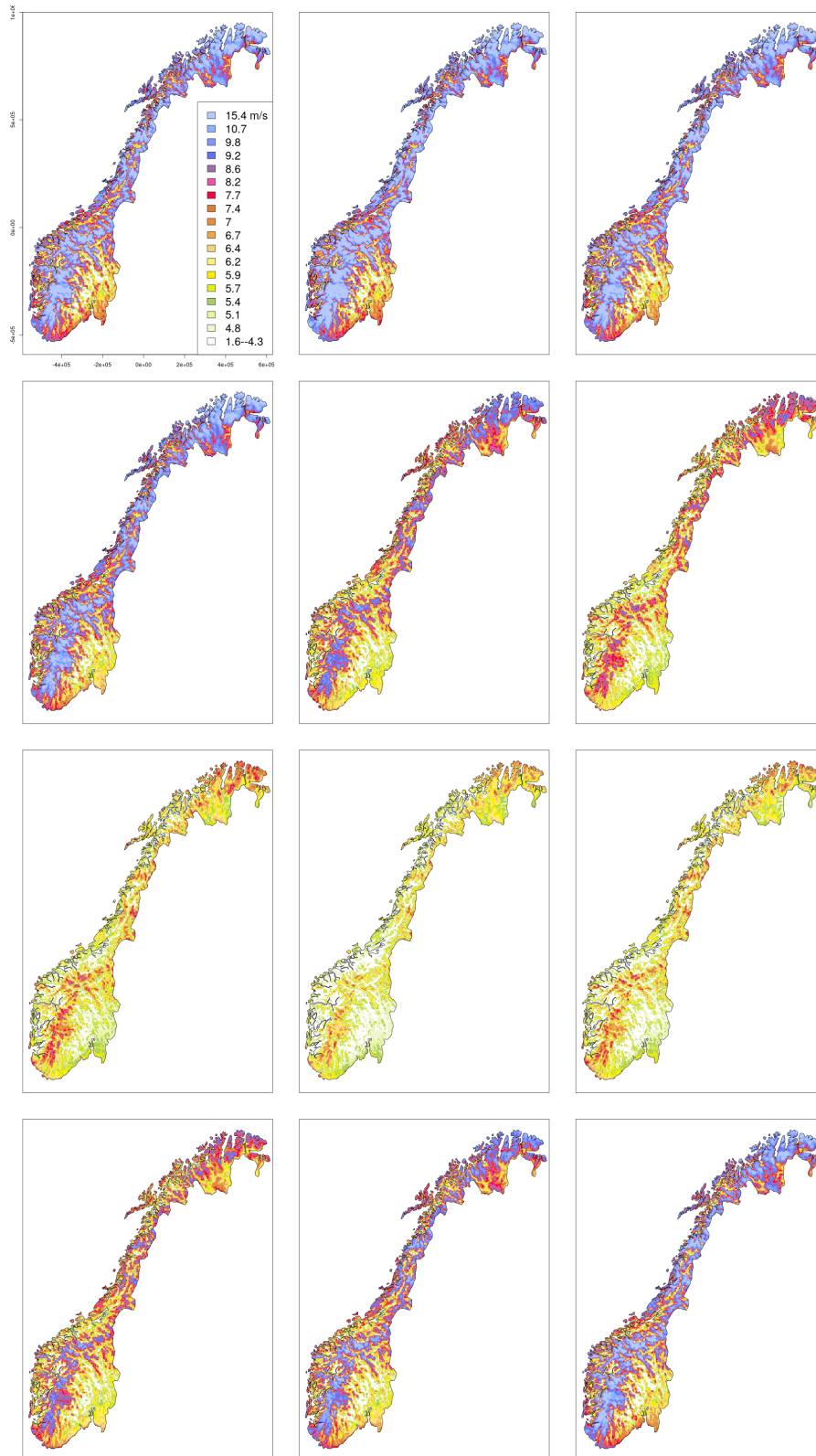


Figure 6: Average 100–metre wind speed 1991–2020 monthly normals. Winter months in the top row (left to right): Dec, Jan, Feb (or DJF). Spring in the 2nd row (MAM). Summer in the 3rd row (JJA). Autumn in the bottom row (SON).

3.2.1 Temporal trends

The results are presented in the figures that follows, either in this section or in the supporting material (SFigs. 41– 86). For convenience, the list of available figures is shown below:

- Fig. 7. Normalized linear trends of the monthly averaged 10–metre wind speed over the period 1991-2020. Each of the 30 annual values was derived from NORA3 hourly 10–metre wind speed.
- Fig. 8. Normalized linear trends of the monthly averaged 100–metre wind speed over the period 1991-2020. Each of the 30 annual values was derived from NORA3 hourly 100–metre wind speed.

The layout of the maps in the figures is similar to that described in Sec. 3.1.1. In Figs. 9- 10 the only two months where the trends of the 10–m wind speed are significant at level 10% are shown.

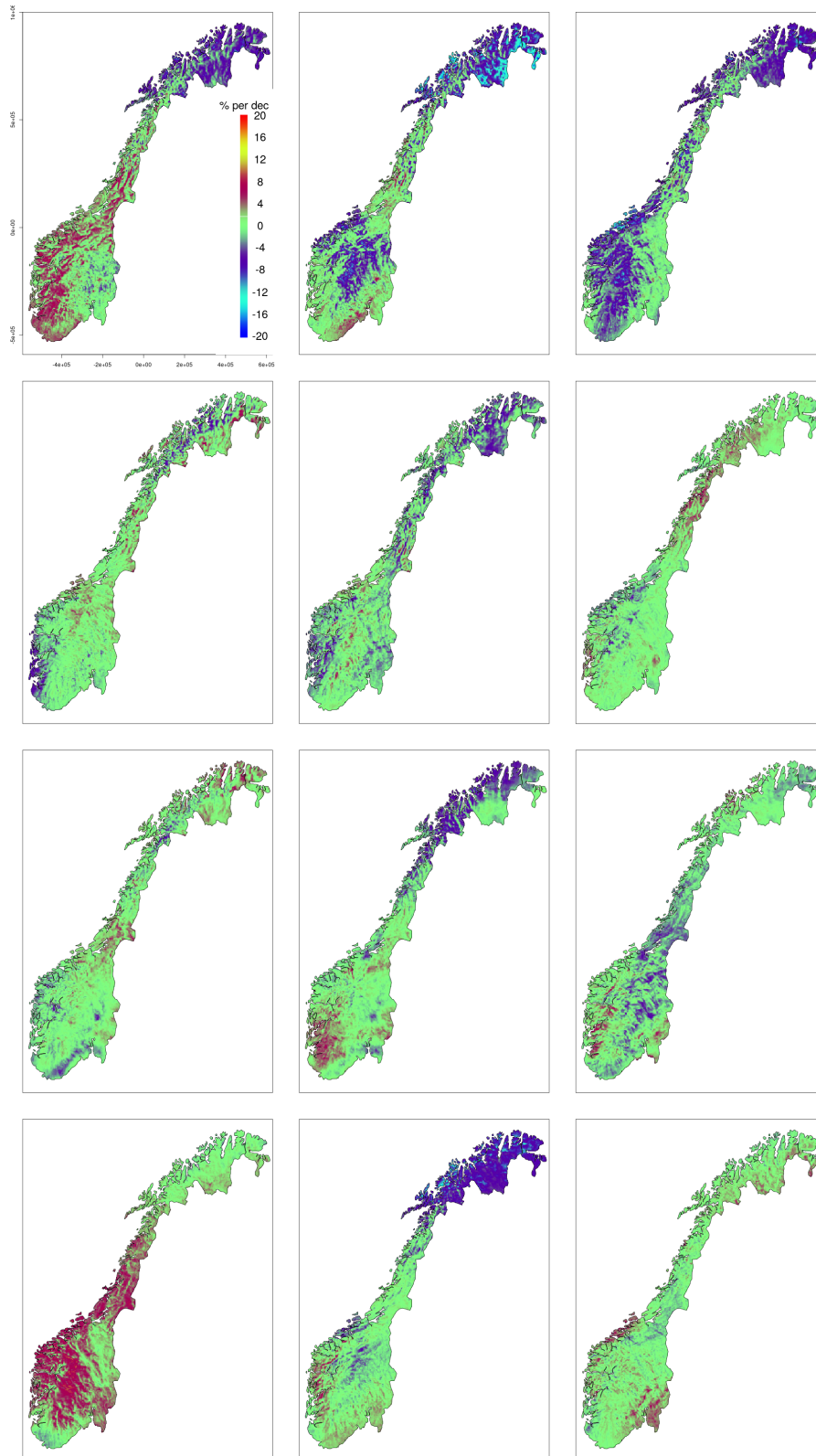


Figure 7: Normalized linear trends (in % of the climate normals per decade) of the monthly averaged 10-metre wind speed over the period 1991-2020. Winter months in the top row (left to right): Dec, Jan, Feb (or DJF). Spring in the 2nd row (MAM). Summer in the 3rd row (JJA). Autumn in the bottom row (SON).

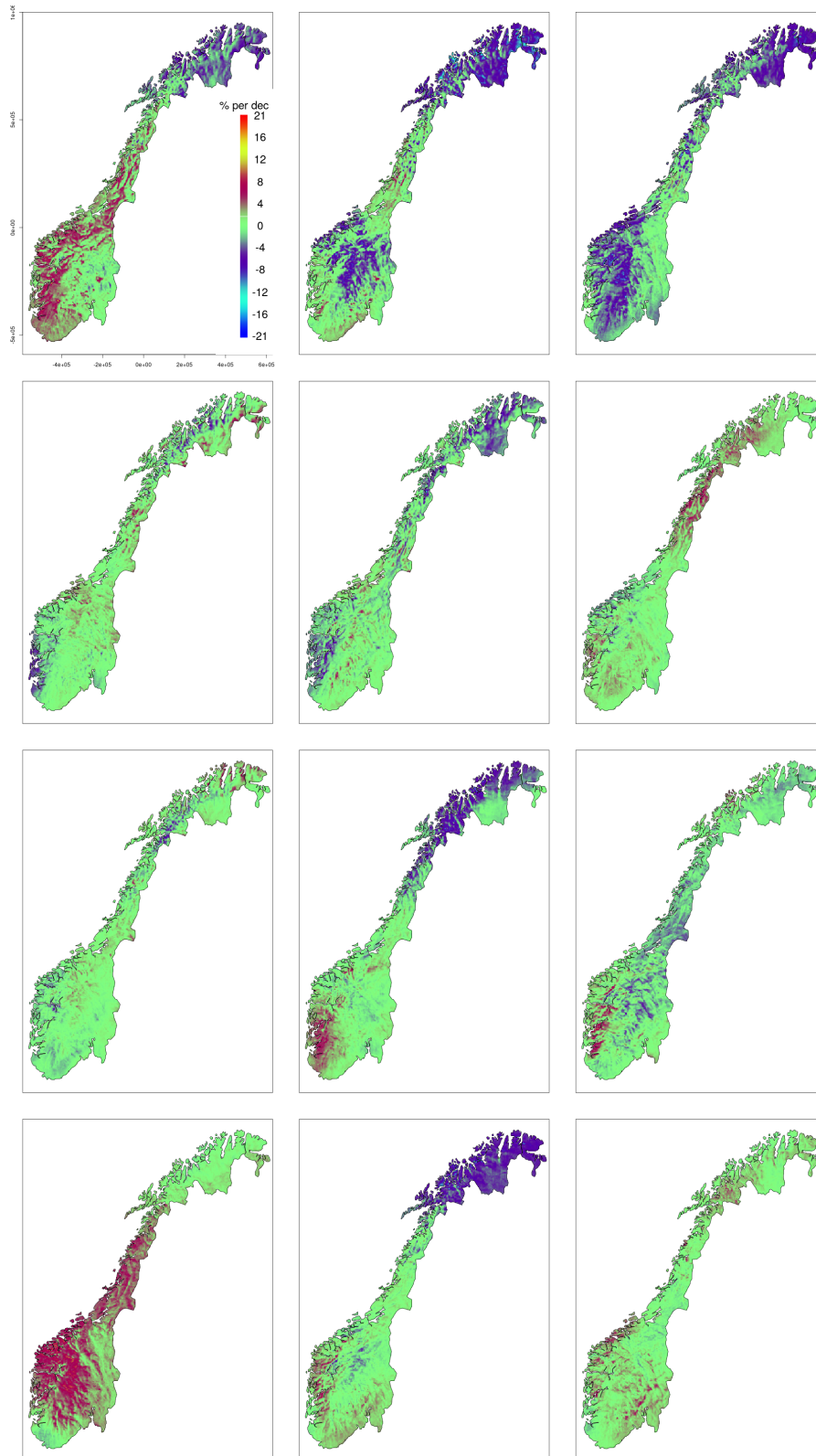


Figure 8: Normalized linear trends (in % of the climate normals per decade) of the monthly averaged 100–metre wind speed over the period 1991–2020. Winter months in the top row (left to right): Dec, Jan, Feb (or DJF). Spring in the 2nd row (MAM). Summer in the 3rd row (JJA). Autumn in the bottom row (SON).

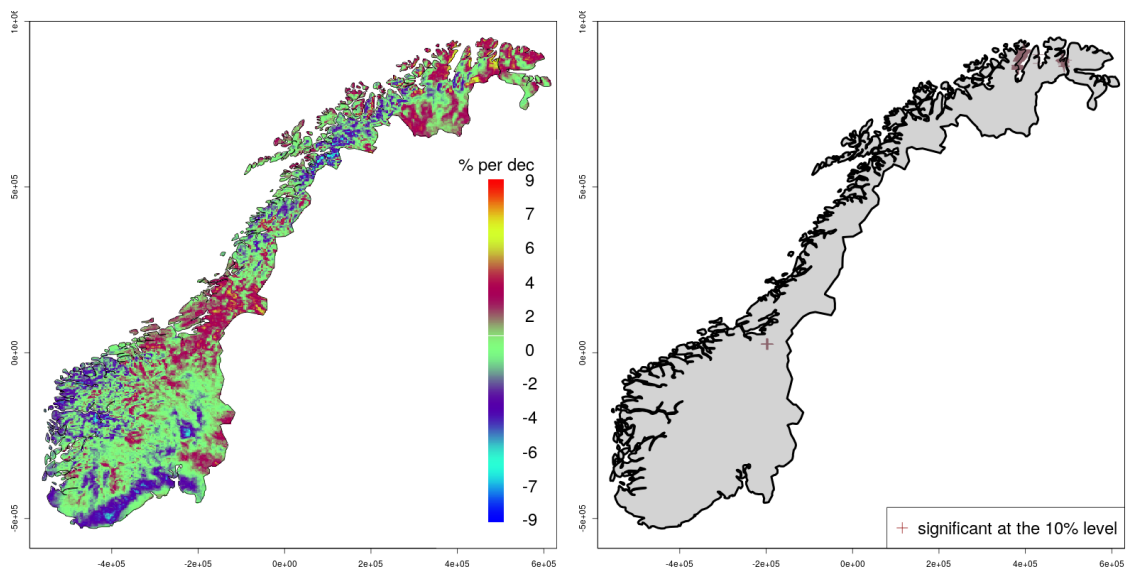


Figure 9: Normalized linear trends (in % of the climate normals per decade) of the monthly averaged 10–metre wind speed for the month of June over the period 1991-2020. At a grid point, each of the 30 monthly values used was derived from NORA3 hourly 10–metre wind speed. The left panel shows the map of the normalized trends. The right panel shows the grid points where the temporal trends are significant at the 10% level.

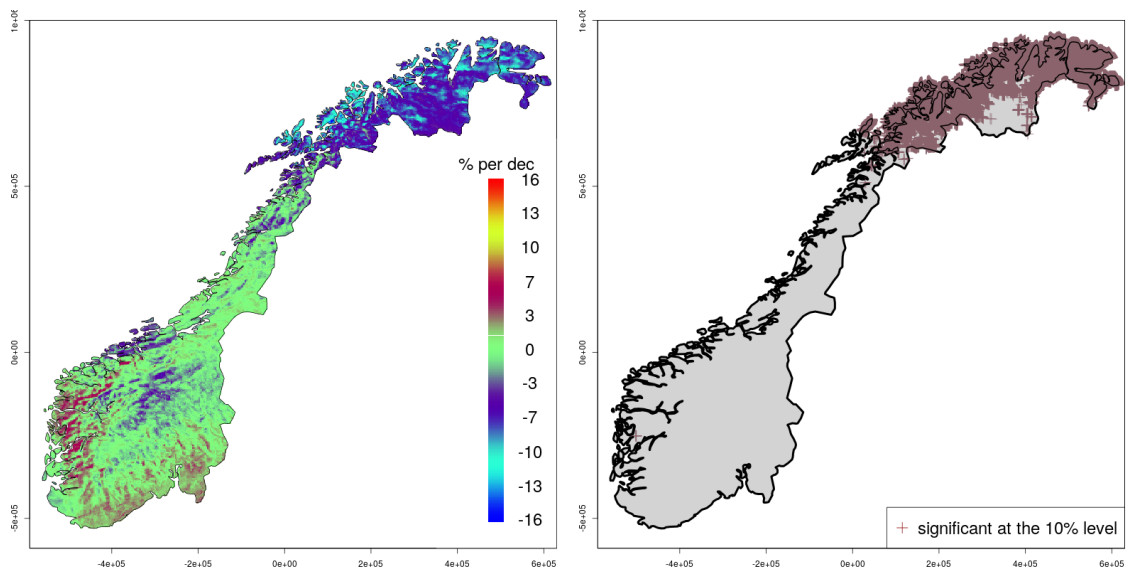


Figure 10: Normalized linear trends (in % of the climate normals per decade) of the monthly averaged 10–metre wind speed for the month of October over the period 1991–2020. At a grid point, each of the 30 monthly values used was derived from NORA3 hourly 10–metre wind speed. The left panel shows the map of the normalized trends. The right panel shows the grid points where the temporal trends are significant at the 10% level.

4 Wind speed climatology over the sea

4.1 Annual aggregated variables

The results are presented in the figures that follows, either in this section or in the supporting material (SFIGs. 87– 92). For convenience, the list of available figures is shown below:

- Fig. 11. Average 10–metre wind speed 1991–2020 normal. Each of the 30 annual values was derived from NORA3 hourly 10–metre wind speed.
- SFIG. 87. 30-year average (1991–2020) of the 99-th percentile of the annual 10–metre wind speed. Each of the 30 annual values was derived from NORA3 on the basis of all daily mean 10–metre wind speeds.
- Fig. 12. Average 100–metre wind speed 1991–2020 normal. Each of the 30 annual values was derived from NORA3 hourly 100–metre wind speed.
- SFIG. 88. 30-year average (1991–2020) of the 99-th percentile of the annual 100–metre wind speed. Each of the 30 annual values was derived from NORA3 on the basis of all daily mean 100–metre wind speeds.
- SFIG. 89. 30-year average (1991–2020) of the number of hours in a year with 10–metre wind speed less than 4 m/s. Each of the 30 annual values was derived from NORA3 on the basis of all hourly 10–metre wind speeds.
- SFIG. 90. 30-year average (1991–2020) of the number of hours in a year with 10–metre wind speed greater than 25 m/s. Each of the 30 annual values was derived from NORA3 on the basis of all hourly 10–metre wind speeds.
- SFIG. 91. 30-year average (1991–2020) of the number of hours in a year with 100–metre wind speed less than 4 m/s. Each of the 30 annual values was derived from NORA3 on the basis of all hourly 100–metre wind speeds.
- SFIG. 92. 30-year average (1991–2020) of the number of hours in a year with 100–metre wind speed greater than 25 m/s. Each of the 30 annual values was derived from NORA3 on the basis of all hourly 100–metre wind speeds.

The layout of all figures is the same. The left panel shows a map with the field of the normal values over a regular grid with spacing of 1 km. The colour scale is defined on the basis of the percentiles of the distribution of values as in Sec. 3.1.

The right panel shows the histogram of the distribution of the normal values that are shown in the left panel.

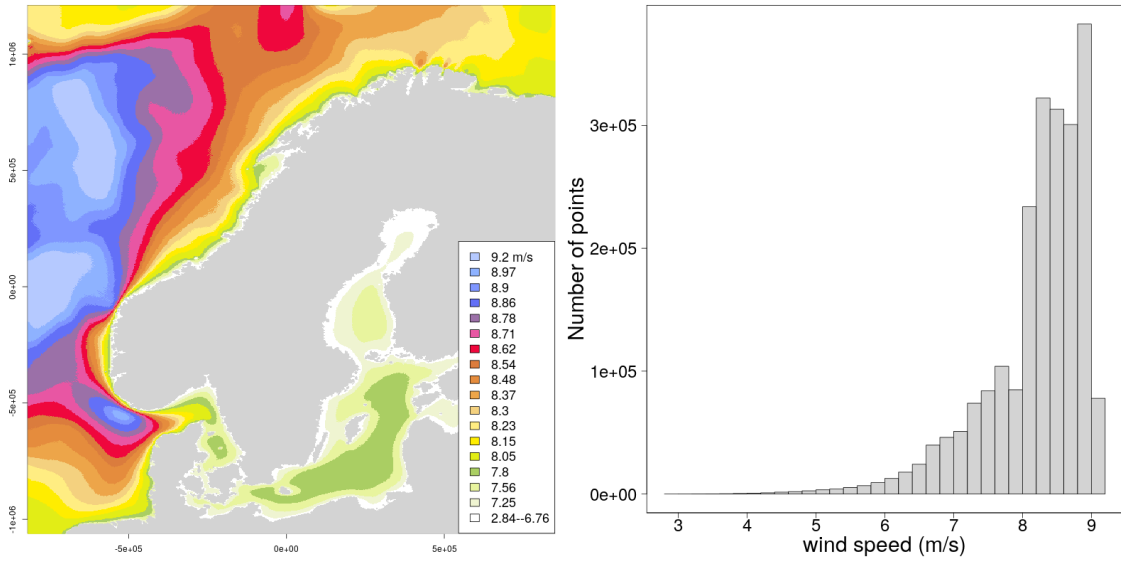


Figure 11: Average 10–metre wind speed 1991–2020 normal. Each of the 30 annual values was derived from NORA3 hourly 10–metre wind speed.

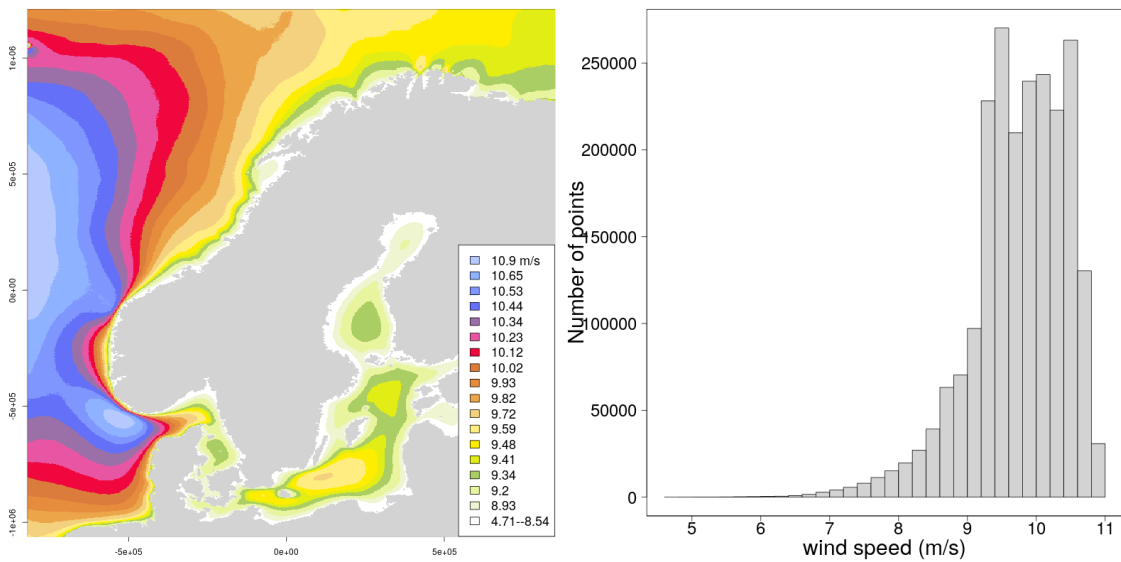


Figure 12: Average 100–metre wind speed 1991–2020 normal. Each of the 30 annual values was derived from NORA3 hourly 100–metre wind speed.

4.1.1 Temporal trends

The results are presented in the figures that follows, either in this section or in the supporting material (SFIGs. 93– 94). For convenience, the list of available figures is shown below:

- Fig. 13. Normalized linear trends of the annual averaged 10–metre wind speed over the period 1991-2020. At a grid point, each of the 30 annual values used was derived from NORA3 hourly 10–metre wind speed.
- SFIG. 93. Normalized linear trends of the annual 99-th percentile of the 10–metre wind speed over the period 1991-2020. At a grid point, each of the 30 annual values used was derived from NORA3 daily averaged 10–metre wind speed.
- SFIG. 94. Normalized linear trends of the annual averaged 100–metre wind speed over the period 1991-2020. At a grid point, each of the 30 annual values used was derived from NORA3 hourly 100–metre wind speed.
- Fig. 14. Normalized linear trends of the annual 99-th percentile of the 100–metre wind speed over the period 1991-2020. At a grid point, each of the 30 annual values used was derived from NORA3 daily averaged 100–metre wind speed.

The layout of the figures is the same as in Sec. 3.1.1.

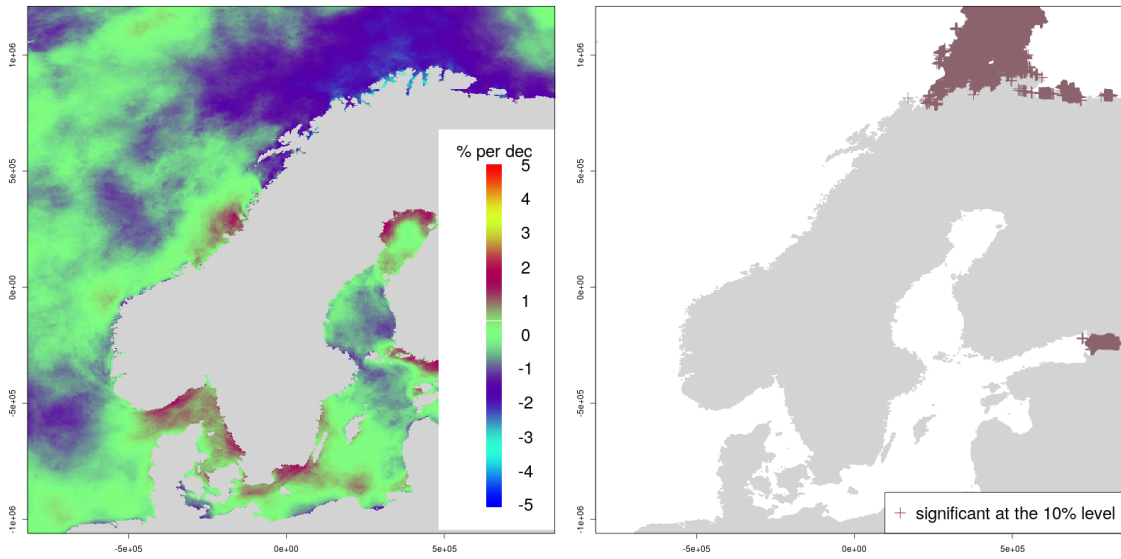


Figure 13: Normalized linear trends (in % of the climate normals per decade) of the annual averaged 10–metre wind speed over the period 1991-2020. At a grid point, each of the 30 annual values used was derived from NORA3 hourly 10–metre wind speed. The left panel shows the map of the normalized trends. The right panel shows the grid points where the temporal trends are significant at the 10% level.

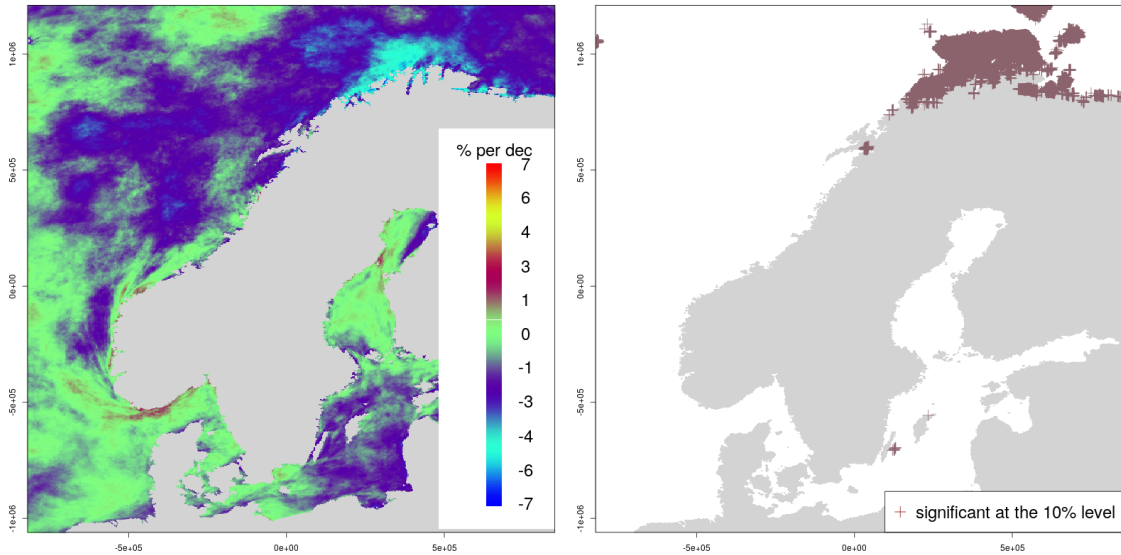


Figure 14: Normalized linear trends (in % of the climate normals per decade) of the annual 99-th percentile of the 100–metre wind speed over the period 1991-2020. At a grid point, each of the 30 annual values used was derived from NORA3 daily averaged 100–metre wind speed. The left panel shows the map of the normalized trends. The right panel shows the grid points where the temporal trends are significant at the 10% level.

4.2 Monthly aggregated variables

The results are presented in the figures that follows, either in this section or in the supporting material (SFigs. 95– 102). For convenience, the list of available figures is shown below:

- Fig. 15. Average 10–metre wind speed 1991–2020 monthly normals. Each of the 30 annual values was derived from NORA3 hourly 10–metre wind speed.
- Fig. 16. Average 100–metre wind speed 1991–2020 monthly normals. Each of the 30 annual values was derived from NORA3 hourly 10–metre wind speed.

The layout of the figures is similar to those of the maps in Sec. 3.1.

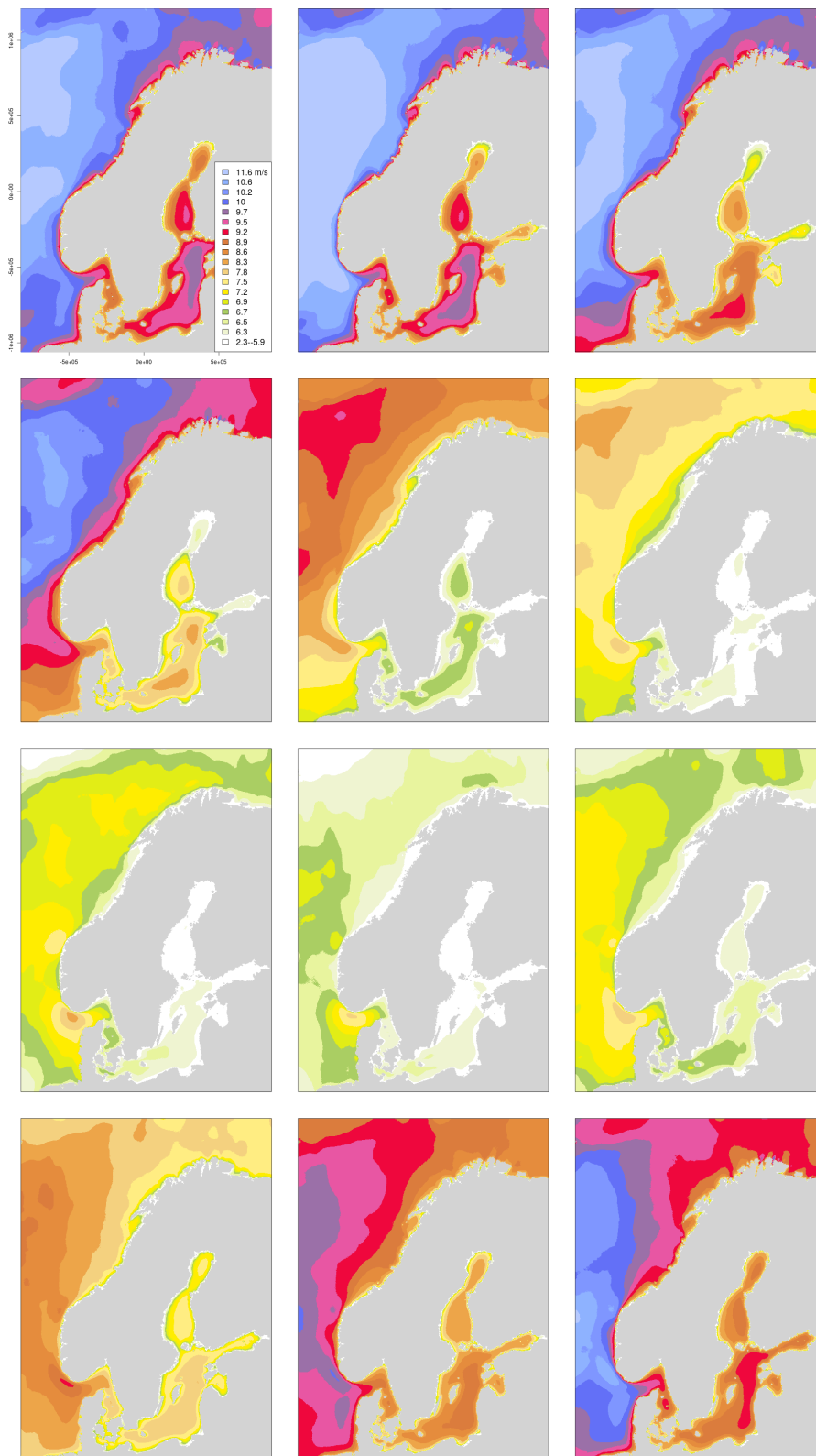


Figure 15: Average 10-metre wind speed 1991–2020 monthly normals. Winter months in the top row (left to right): Dec, Jan, Feb (or DJF). Spring in the 2nd row (MAM). Summer in the 3rd row (JJA). Autumn in the bottom row (SON).

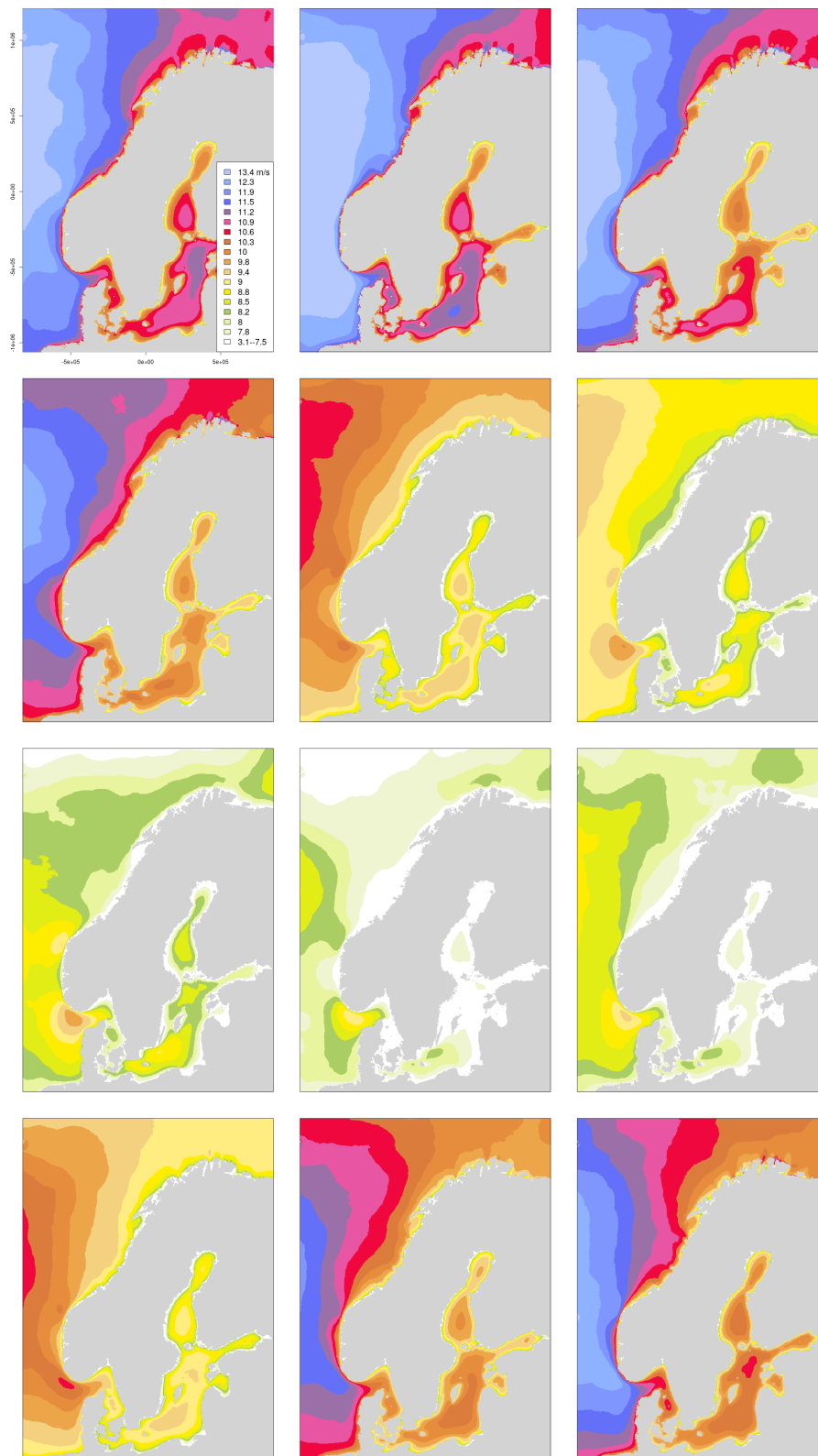


Figure 16: Average 100–metre wind speed 1991–2020 monthly normals. Winter months in the top row (left to right): Dec, Jan, Feb (or DJF). Spring in the 2nd row (MAM). Summer in the 3rd row (JJA). Autumn in the bottom row (SON).

4.2.1 Temporal trends

The results are presented in the figures that follows, either in this section or in the supporting material (SFigs. 103– 124). For convenience, the list of available figures is shown below:

- Fig. 17. Normalized linear trends of the monthly averaged 10–metre wind speed over the period 1991-2020. Each of the 30 annual values was derived from NORA3 hourly 10–metre wind speed.
- Fig. 18. Normalized linear trends of the monthly averaged 100–metre wind speed over the period 1991-2020. Each of the 30 annual values was derived from NORA3 hourly 100–metre wind speed.

The layout of the maps in the figures is similar to that described in Sec. 3.1.1. In Figs. 19- 20 the only two months where the trends of the 10–m wind speed are significant at level 10% are shown.

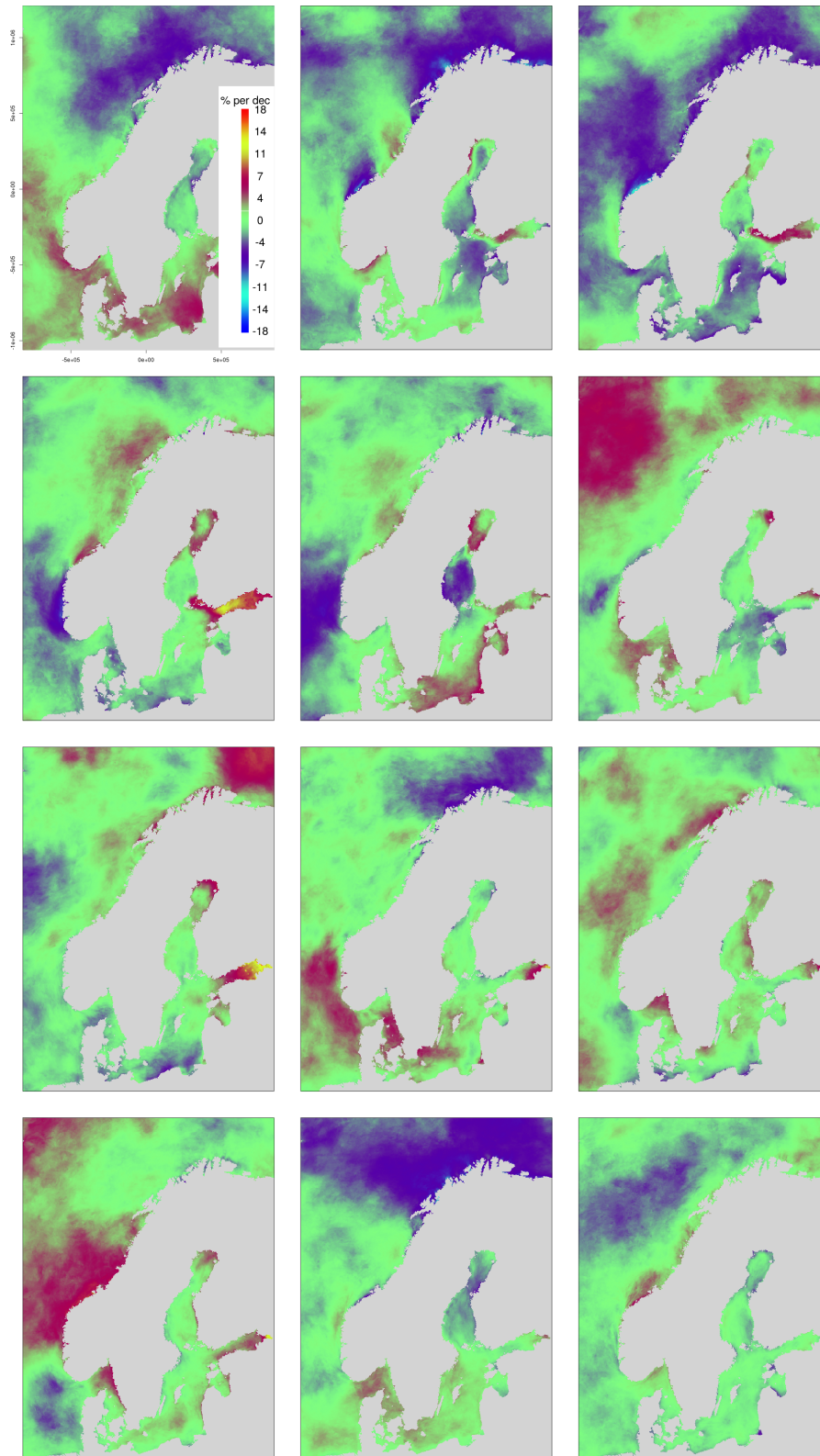


Figure 17: Normalized linear trends (in % of the climate normals per decade) of the monthly averaged 10-metre wind speed over the period 1991-2020. Winter months in the top row (left to right): Dec, Jan, Feb (or DJF). Spring in the 2nd row (MAM). Summer in the 3rd row (JJA). Autumn in the bottom row (SON).

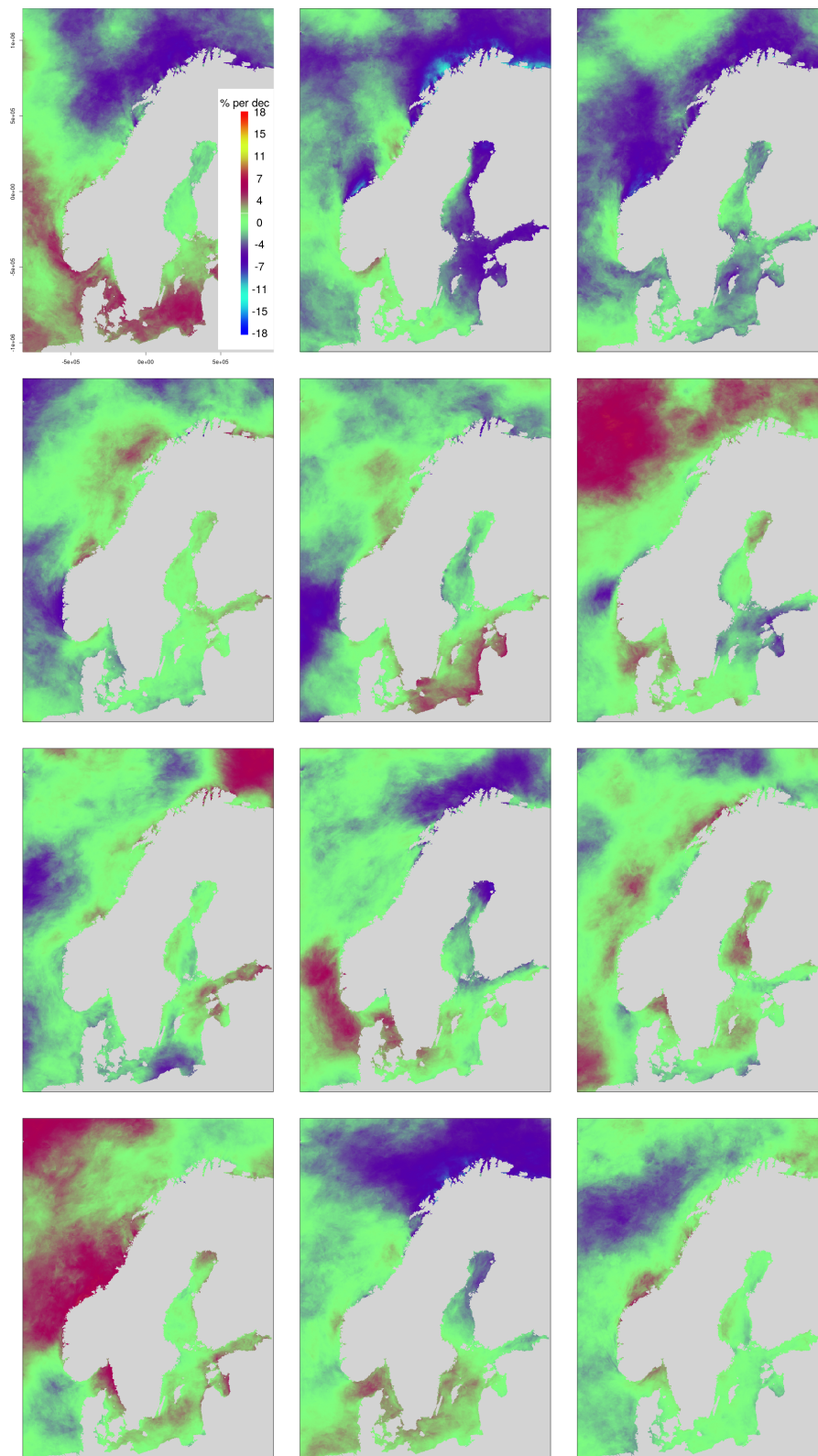


Figure 18: Normalized linear trends (in % of the climate normals per decade) of the monthly averaged 100–metre wind speed over the period 1991–2020. Winter months in the top row (left to right): Dec, Jan, Feb (or DJF). Spring in the 2nd row (MAM). Summer in the 3rd row (JJA). Autumn in the bottom row (SON).

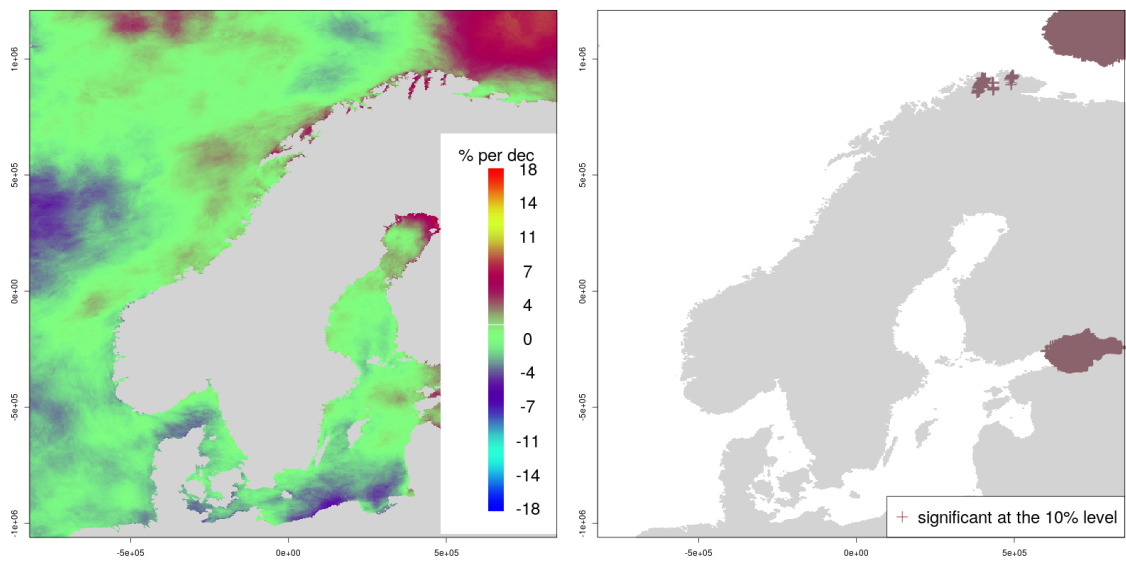


Figure 19: Normalized linear trends (in % of the climate normals per decade) of the monthly averaged 10–metre wind speed for the month of June over the period 1991–2020. At a grid point, each of the 30 monthly values used was derived from NORA3 hourly 10–metre wind speed. The left panel shows the map of the normalized trends. The right panel shows the grid points where the temporal trends are significant at the 10% level.

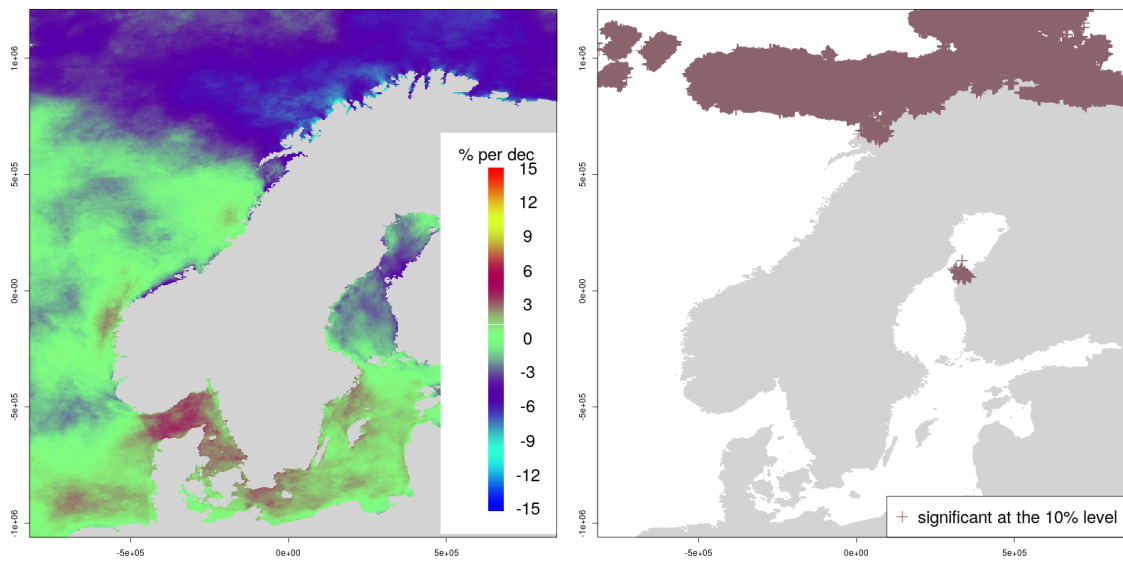


Figure 20: Normalized linear trends (in % of the climate normals per decade) of the monthly averaged 10–metre wind speed for the month of October over the period 1991–2020. At a grid point, each of the 30 monthly values used was derived from NORA3 hourly 10–metre wind speed. The left panel shows the map of the normalized trends. The right panel shows the grid points where the temporal trends are significant at the 10% level.

5 Conclusions

NORA3 provides high resolution wind speed fields over a large domain. The 10-m wind speed monthly and yearly aggregated data agrees reasonably well with the observed data, as can be seen from the numerous graphs where NORA3 values have been compared against in-situ observations from selected stations of the MET Norway network (see the supporting material: SFigs. 9–32 for annual values; SFigs.63–86 for monthly values).

The 1991–2020 climatology over the Norwegian mainland shows that the strongest winds occurs in the mountains and along the coast of Troms og Finmark in Northern Norway, while Eastern Norway is the region where the wind is generally less intense because it lies in the leeward side of the Scandinavian mountains. The climatology over the sea shows that the strongest winds occur in the Norwegian Sea, off the coast of Western Norway.

The wind speed has a distinct seasonal cycle and the average wind is stronger in winter and weaker in summer. Thanks to the fine spatial resolution achievable using NORA3, the distributions of wind speed values at 10-m and 100-m elevations are presented on a high resolution grid both for the normal values and for the typical values of the strongest winds.

The interannual variability of wind speed makes it difficult to find significant temporal trends in the wind speed. The main climatological signals, which are statistically significant, are observed in the Troms og Finmark region and in the region between the northern part of the Norwegian sea and the Barents sea. They consist of a reduction in both the average 10-m wind speed and the 99-th percentile of the 100-metre wind speed. As for the monthly aggregated values, these climatological trends seem to be more evident in the month of October.

Appendix: Data Access

The original NORA3 data used in our study are openly available at:

- <https://thredds.met.no/thredds/catalog/nora3/catalog.html>

The directory structure is organized in year/month/day. For each day, there are four model runs depending on the initialization time: 00:00 UTC, 06:00 UTC, 12:00 UTC and 18:00 UTC. The files we have used are those having filenames like:

- `fc%Y%m%d%H_%F_fp.nc`

where: %Y%m%d is the date of the run; %H is the initialization time; %F is the forecast lead time. The files to be used have lead time forecasts ranging from 004 to 009. These files include wind speed at 10-m and also `x_wind_z` and `y_wind_z` at 100-m.

The NORA3 post-processed gridded datasets used in this report can be obtained by contacting Cristian Lussana (cristian.lussana@met.no).

References

- Haakenstad, H., Øyvind Breivik, B. R. Furevik, M. Reistad, P. Bohlinger, and O. J. Aarnes (2021), Nora3: A nonhydrostatic high-resolution hindcast of the north sea, the norwegian sea, and the barents sea, *Journal of Applied Meteorology and Climatology*, 60(10), 1443 – 1464, doi:10.1175/JAMC-D-21-0029.1.
- Hersbach, H., B. Bell, P. Berrisford, S. Hirahara, A. Horányi, J. Muñoz-Sabater, J. Nicolas, C. Peubey, R. Radu, D. Schepers, A. Simmons, C. Soci, S. Abdalla, X. Abellan, G. Balsamo, P. Bechtold, G. Biavati, J. Bidlot, M. Bonavita, G. De Chiara, P. Dahlgren, D. Dee, M. Diamantakis, R. Dragani, J. Flemming, R. Forbes, M. Fuentes, A. Geer, L. Haimberger, S. Healy, R. J. Hogan, E. Hólm, M. Janisková, S. Keeley, P. Laloyaux, P. Lopez, C. Lupu, G. Radnoti, P. de Rosnay, I. Rozum, F. Vamborg, S. Villaume, and J.-N. Thépaut (2020), The era5 global reanalysis, *Quarterly Journal of the Royal Meteorological Society*, 146(730), 1999–2049, doi:<https://doi.org/10.1002/qj.3803>.
- Lanzante, J. R. (1996), Resistant, robust and non-parametric techniques for the analysis of climate data: theory and examples, including applications to historical radiosonde station data, *International Journal of Climatology*, 16(11), 1197–1226.
- Wilks, D. S. (2019), *Statistical methods in the atmospheric sciences (Fourth Edition)*, fourth edition ed., Elsevier, doi:<https://doi.org/10.1016/B978-0-12-815823-4.00009-2>.